

PHYSICAL REVIEW D

PARTICLES AND FIELDS

THIRD SERIES, VOLUME 45, NUMBER 7

1 APRIL 1992

RAPID COMMUNICATIONS

Rapid Communications are intended for important new results which deserve accelerated publication, and are therefore given priority in editorial processing and production. A Rapid Communication in Physical Review D should be no longer than five printed pages and must be accompanied by an abstract. Page proofs are sent to authors, but because of the accelerated schedule, publication is generally not delayed for receipt of corrections unless requested by the author.

Study of the decays $D \rightarrow K\pi\pi\nu$ and $D \rightarrow K^*\pi\nu$

J. C. Anjos,^c J. A. Appel,^f A. Bean,^a S. B. Bracker,^k T. E. Browder,^{a,*} L. M. Cremaldi,^g J. E. Duboscq,^a J. R. Elliott,^{e,†} C. O. Escobar,^j M. C. Gibney,^{e,‡} G. F. Hartner,^k J. Huber,^a P. E. Karchin,^l B. R. Kumar,^k M. J. Losty,^h G. J. Luste,^k P. M. Mantsch,^f J. F. Martin,^k S. McHugh,^a S. R. Menary,^{k,§} R. J. Morrison,^a T. Nash,^f J. Pinfold,^b G. Punkar,^a M. V. Purohit,ⁱ W. R. Ross,^l A. F. S. Santoro,^c D. M. Schmidt,^a A. L. Shoup,^d K. Sliwa,^{f,**} M. D. Sokoloff,^d M. H. G. Souza,^c D. J. Sperka,^a M. E. Streetman,^f A. B. Stundžia,^k and M. S. Witherell^a

^aUniversity of California, Santa Barbara, California 93106

^bCarleton University, Ottawa, Ontario, Canada K1S 5B6

^cCentro Brasileiro de Pesquisas Físicas, Rio de Janeiro, Brazil

^dUniversity of Cincinnati, Cincinnati, Ohio 45221

^eUniversity of Colorado, Boulder, Colorado 80309

^fFermi National Accelerator Laboratory, Batavia, Illinois 60510

^gUniversity of Mississippi, Oxford, Mississippi 38677

^hNational Research Council, Ottawa, Ontario, Canada K1A 0R6

ⁱPrinceton University, Princeton, New Jersey 08544

^jUniversidade de São Paulo, São Paulo, Brazil

^kUniversity of Toronto, Toronto, Ontario, Canada M5S 1A7

^lYale University, New Haven, Connecticut 06511

(Received 29 October 1991)

We have searched for the exclusive semileptonic decay modes $D^+ \rightarrow \bar{K}\pi\pi^+\nu_e$ and $D^+ \rightarrow \bar{K}^*\pi^+\nu_e$ in the data from the Fermilab photoproduction experiment E691. With good sensitivity, we observe no signals in the channels $D^+ \rightarrow K^-\pi^+\pi^0e^+\nu_e$ and $D^+ \rightarrow \bar{K}^0\pi^+\pi^-e^+\nu_e$, and set upper limits of $B(D^+ \rightarrow \text{all } \bar{K}^*\pi^+\nu_e) < 1.2\%$ and $B(D^+ \rightarrow \text{all } \bar{K}\pi\pi^+\nu_e) < 0.9\%$, at the 90% confidence level. (For these limits we use isospin invariance to extract limits which include all charge states.) These modes are expected to be the most common semileptonic decays next to the dominant $\bar{K}e^+\nu_e$ and $\bar{K}^*e^+\nu_e$, but the observed limits represent a small fraction of the inclusive semileptonic branching ratio of $(17.0 \pm 1.9 \pm 1.7)\%$.

PACS number(s): 13.20.Fc, 14.40.Jz

*Now at Cornell University, Ithaca, NY 14853.

†Now at Electromagnetic Applications, Inc., Denver, CO 80226.

‡Now at Nichols Research Inc., Colorado Springs, CO 80919.

§Now at CERN, EP Division, CH-1211 Genève, Switzerland.

**Now at Tufts University, Medford, MA 02155.

INTRODUCTION

The heavy-quark decays that are both accessible experimentally and the simplest to interpret theoretically are the exclusive semileptonic decays. Such decays proceed through spectator processes, and the strong-

TABLE I. Summary of exclusive and inclusive charm decay rates.

Mode	Source	Decay width (10^{10} s^{-1})
$D \rightarrow K e \nu$	E691	7.3 ± 1.2
$D \rightarrow K^* e \nu$	E691	4.0 ± 0.8
$D \rightarrow (K\pi)_{\text{NRE}} e \nu$	E691	0.4 ± 0.4
$D \rightarrow (\pi, \rho) e \nu$	V_{cd}/V_{cs}	0.9 ± 0.3
Total		12.6 ± 1.5
$D \rightarrow X e \nu$	Mark III av [1]	16.5 ± 1.6
Missing decays		3.9 ± 2.2

interaction effects are completely contained in the form factors. They are therefore used to measure the Cabibbo-Kobayashi-Maskawa (CKM) matrix elements which relate the weak-interaction quark eigenstates to the strong ones. There is a large theoretical effort to calculate the form factors; these form-factor models can be checked in $c \rightarrow s e \nu_e$ decays, since the CKM element V_{cs} is well known. In current theoretical models, the lowest-mass resonances K and K^* almost saturate the $c \rightarrow s e \nu_e$ rate. Experimentally, there is room for a large contribution from higher resonances, however. The total of the exclusive decay rates shown in Table I is $(12.6 \pm 1.5) \times 10^{10} \text{ s}^{-1}$, compared to $(16.5 \pm 1.6) \times 10^{10} \text{ s}^{-1}$ for the inclusive rate from Mark III [1]. The rate for missing decays of $(3.9 \pm 2.2) \times 10^{10} \text{ s}^{-1}$ is consistent within errors both with zero and with the rate of the major decays.

To try to reduce the uncertainty in the size of the contributions from higher K^* resonances, we searched directly for the exclusive decay modes $D \rightarrow K \pi \pi e \nu_e$ and $D \rightarrow K^* \pi e \nu_e$, which are expected to be the largest remaining modes. We analyzed data from the Fermilab charm photoproduction experiment E691 already used to measure $D \rightarrow K e \nu$ [2,3] and $D \rightarrow K^* e \nu$ [4,5] decay modes. The detector is a two-magnet spectrometer with large acceptance, good mass resolution, particle identification, and a high-resolution silicon microstrip detector. The silicon microstrip detector and the spectrometer have been previously described in detail [6].

$D^+ \rightarrow K^- \pi^+ \pi^0 e^+ \nu_e$ ANALYSIS

We used the same $K^- \pi^+ e^+$ sample previously used to study the $D^+ \rightarrow \bar{K}^{*0} e^+ \nu_e$ decay [4,5] to look for $K^- \pi^+ \pi^0 e^+ \nu_e$ (including $\bar{K}^* \pi e^+ \nu_e$). We did not require the π^0 to be detected. We required well identified electrons with an electron probability corresponding to a typical efficiency for electrons and pions of 61% and 0.3%, respectively. We eliminated electrons visibly resulting from secondary photon conversion, electrons consistent with beam photon pair conversions, and those with energy less than 12 GeV.

The $\bar{K} \pi e$ candidates were selected using only tracks seen in both the drift chambers and the silicon microstrip detectors. Only well identified neutral $\bar{K} \pi$ combinations were used; combinations in which the kaon and the

electron have opposite (same) charges are labeled right- (wrong-) sign combinations. The electron and kaon were required to pass through both detector magnets. The vertex cuts were those used for the earlier $\bar{K}^{*0} e^+ \nu_e$ analysis [4,5].

The χ^2 per degree of freedom of the $\bar{K} \pi e$ secondary vertex was required to be less than 3.5. The kaon, pion, and electron tracks originated from a secondary vertex which was separated from the primary vertex by 10 standard deviations plus the distance corresponding to a 0.2-ps proper decay time. The $\bar{K} \pi e$ line of flight pointed back to the primary vertex within 2.5 times the resolution plus the maximum displacement due to the missing neutrino and π^0 . No candidates with an extra track within 65 μm of the secondary vertex were accepted, and all decay tracks were closer to the secondary vertex than any other vertex. We eliminated events consistent with $D^{*+} \rightarrow \pi^+ D^0 (D^0 \rightarrow K^- e^+ \nu_e)$ and misidentified $D^+ \rightarrow K^- \pi^+ \pi^+$ decays.

We made two-dimensional maximum-likelihood fits to the $\bar{K} \pi$ and $\bar{K} \pi e$ mass spectrum for the resulting 313 right-sign and 62 wrong-sign events. This made full use of the characteristics that separate the $\bar{K} \pi \pi e \nu$ decay from the dominant $\bar{K}^* e \nu$ events. For the analysis of $D^+ \rightarrow \bar{K}^* \pi e^+ \nu_e$, there are two contributions: $K^* \pi^+$ and $\bar{K}^{*0} \pi^0$, which must have equal contributions to the $K^- \pi^+ \pi^0$ final state since the hadronic current in both decays has $I = \frac{1}{2}$. The signal function is a combination of the $D^+ \rightarrow K^* \pi^+ e^+ \nu_e$ and $D^+ \rightarrow \bar{K}^{*0} \pi^0 e^+ \nu_e$ signal functions determined from Monte Carlo studies. Figures 1(a) and 2(a) show the data and fit projections for the combined $K^* \pi e \nu_e$ Monte Carlo events. For the nonresonant $D^+ \rightarrow (K^- \pi^+ \pi^0)_{\text{NRE}} e^+ \nu_e$ signal, we assume that the decay has a constant matrix element. Broad resonances have similar distributions.

The data sample is dominated by the mode $D^+ \rightarrow \bar{K}^{*0} e^+ \nu_e$ where $\bar{K}^{*0} \rightarrow K^- \pi^+$, with the function shape determined using known form factors which were measured using this data set [5]. The wrong-sign events

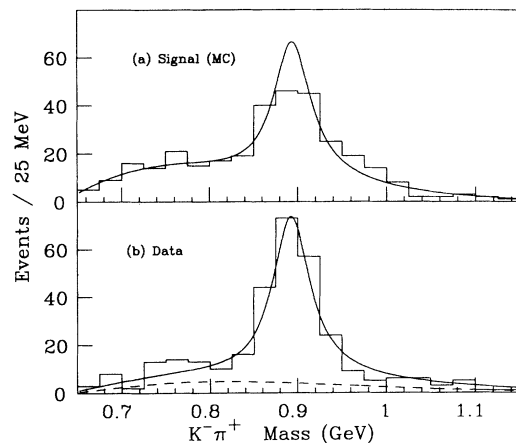


FIG. 1. The $K^- \pi^+$ mass spectrum with right-sign combinations: (a) combined $K^* \pi e \nu_e$ Monte Carlo signal events and (b) data events. The curves are the right-sign (solid lines) and wrong-sign (dashed line) fits described in the text.

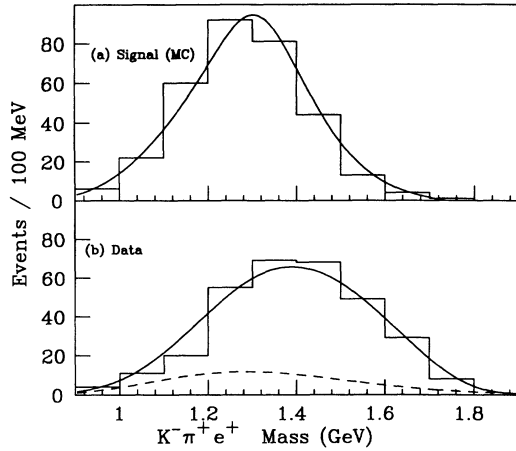


FIG. 2. The $K^-\pi^+e^+$ mass spectrum with right-sign combinations: (a) combined $K^*\pi e\nu$ Monte Carlo signal events, and (b) data events. The curves are the right-sign (solid lines) and wrong-sign (dashed line) fits described in the text.

were shown to be a good measure of the background by looking at data with loose cuts or outside the kinematic region for signal. They are thus used to model the background, and the background fit is shown by the dashed curve in Figs. 1(b) and 2(b). The nonresonant $\bar{K}\pi e\nu$ was modeled using a simple momentum power turn on for the $\bar{K}\pi$ phase space.

The two-dimensional maximum-likelihood fit uses the signal shape, the wrong-sign background shape from the 62 ± 8 background events, the nonresonant $\bar{K}\pi e\nu$ shape, and the feedthrough from the decay $D^+ \rightarrow \bar{K}^{*0}e^+\nu_e$, as discussed above. The $K^-\pi^+$ and $K^-\pi^+e^+$ mass spectrums and fit projections are shown in Figs. 1(b) and 2(b) for the decay $D^+ \rightarrow \bar{K}^*\pi e^+\nu_e$. A signal for $\bar{K}^*\pi e\nu_e$ would be distinguished from the dominant $\bar{K}^*e\nu_e$ signal by an excess of events with $M(K^-\pi^+) < 0.82 \text{ GeV}/c^2$ and $M(K^-\pi^+e^+) < 1.2 \text{ GeV}/c^2$. The $198 \pm 21 \bar{K}^*e\nu_e$ events and the nonresonant $\bar{K}\pi e\nu_e$ contribution of 40 ± 18 events agree, respectively, with the 209 ± 18 and 42 ± 20 events found in the previous $\bar{K}^*e\nu_e$ analysis [4,5]. In the $D^+ \rightarrow \bar{K}^*\pi e^+\nu_e$ mode that motivates this analysis, we find $15 \pm 33 \pm 9$ events, corresponding to 55 events as a 90%-confidence-level upper limit. The systematic error of the number of signal events stems mainly from uncertainty in the background shape (four events), the signal shape (two events) and $\bar{K}\pi e\nu_e$ shape (seven events). We studied a variety of function shapes that were consistent with the background and signal to determine the systematic error; the parameters which characterize the $\bar{K}\pi e\nu_e$ shape were varied widely due to the uncertainty in the matrix element. The detection efficiency used to calculate the branching ratio included a systematic error due to both the uncertainty in the electron efficiency (7%) and the \bar{K}^{*0} polarization (15%). Normalizing this result with our $D^+ \rightarrow K^-\pi^+\pi^+$ sample and using the absolute branching ratio for that mode from Mark III [7] of $(9.1 \pm 1.3 \pm 0.4)\%$, we find the 90%-confidence-level upper limit $B(D^+ \rightarrow \bar{K}^*\pi e^+\nu_e \rightarrow K^-\pi^+\pi^0 e^+\nu_e) < 1.2\%$ which implies a branching ratio $B(D^+ \rightarrow$ all

$\bar{K}^*\pi e^+\nu_e) < 2.6\%$ at the 90%-confidence-level limit.

For $D^+ \rightarrow (K^-\pi^+\pi^0)_{\text{NRE}}^+\nu_e$, a separate fit using a nonresonant signal shape gives $207 \pm 18 \bar{K}^*e\nu_e$ events, $38 \pm 18 \bar{K}\pi e\nu_e$ events, and a $D^+ \rightarrow (K^-\pi^+\pi^0)_{\text{NRE}}^+\nu_e$ signal contribution of $9 \pm 11 \pm 5$ events. This nonresonant result corresponds to a limit of 29 signal events and a branching ratio $B(D^+ \rightarrow (K^-\pi^+\pi^0)_{\text{NRE}}^+\nu) < 0.6\%$ as 90%-confidence-level limits. The limits for the nonresonant decay mode are better than that for the resonant mode for which more of the signal shape is hidden under the large \bar{K}^* from the $D^+ \rightarrow \bar{K}^*e\nu$.

$D^+ \rightarrow \bar{K}^0\pi^+\pi^-e^+\nu_e$ ANALYSIS

We made similar analysis cuts in our search for $D^+ \rightarrow \bar{K}^0\pi^+\pi^-e^+\nu_e$. The $\bar{K}\pi\pi e$ combinations with oppositely charged pions are called right sign, whereas the $\bar{K}\pi\pi e$ combinations in which the two pions have the same sign charge and the pion and electron have the same (opposite) charges are labeled same- (wrong-) sign combinations. The electron identification requirements were the same as in the previous analysis. The pions and electron were required to pass through both detector magnets with energy greater than 3 and 12 GeV, respectively. The χ^2 per degree of freedom of the electron-pion vertex had to be less than 3.

The \bar{K}^0 sample was observed in the channel $K_S \rightarrow \pi^+\pi^-$, with the pion tracks seen in the drift chambers but not in the microstrip detectors. The combined pion Čerenkov probability was required to be greater than 0.05, and their effective mass to be between 0.480 and 0.514 GeV. The transverse momentum of $\bar{K}^0\pi\pi e$ had to be greater than 0.6 GeV. The two pion and electron tracks originated from a secondary vertex which was separated from the primary vertex by 24 standard deviations, and the $\bar{K}\pi\pi e$ line of flight pointed back to within $80 \mu\text{m}$ of the primary vertex. Other vertex cuts were similar to the previous analysis.

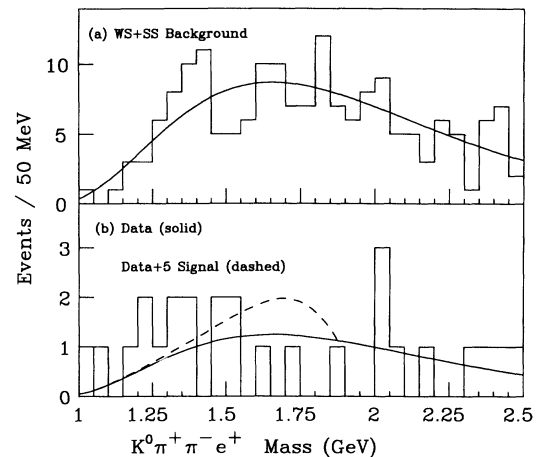


FIG. 3. The $\bar{K}^0\pi^+\pi^-e^+$ mass spectrum for (a) wrong-sign and same-sign combinations and (b) right-sign combinations. The curves are the right-sign (solid lines) and right-sign plus five signal events (dashed line) fits described in the text.

TABLE II. Upper limits at 90% confidence level for $D \rightarrow K\pi\pi\nu_e$ branching ratios, in percent. Isospin constraints are used to calculate limits for all $K^*\pi$ and all $K\pi\pi$ (including $K^-\pi^+\pi^0$, $\bar{K}^0\pi^+\pi^-$, and $\bar{K}^0\pi^0\pi^0$). Here $K\pi\pi$ means either nonresonant $K\pi\pi$ or broad resonances, such as $K\rho$.

Mode	$K^*\pi\nu_e \rightarrow \text{mode}$	All $K^*\pi\nu_e$	$K\pi\pi\nu_e \rightarrow \text{mode}$	All $K\pi\pi\nu_e$
$K^-\pi^+\pi^0e^+\nu_e$	< 1.2	< 2.6	< 0.6	
$K^0\pi^+\pi^-e^+\nu_e$	< 0.5	< 1.2	< 0.5	
Both		< 1.2		< 0.9

The signal shape was modeled from right-sign Monte Carlo events, as shown in Fig. 3(b). The background shape was determined using the wrong-sign and same-sign data events, with a reduced requirement on the secondary to primary vertex separation of at least 6 standard deviations (to produce a larger fit sample). The shape of wrong-sign and same-sign data events agreed with each other, and they were added to produce the background sample. The wrong-sign and same-sign data and the fit are shown in Fig. 3(a).

The right-sign data was fit using the signal and background shape and gave $0.0 \pm 1.7 \pm 2.6$ $D^+ \rightarrow \bar{K}^0\pi^+\pi^- \times e^+\nu_e$ events, or fewer than 5.0 signal events at a 90%-confidence-level limit, as shown in Fig. 3(b). The detection efficiency used to calculate the branching ratio included a systematic error due to both the uncertainty in the electron efficiency (7%) and the \bar{K}^0 efficiency (8.5%). We use our $D \rightarrow K^-\pi^+\pi^+$ sample and the absolute branching ratio for that mode from Mark III to normalize this result, finding the 90%-confidence-level upper limit of $B(D^+ \rightarrow \bar{K}^0\pi^+\pi^-e^+\nu_e) < 0.5\%$. We also use this limit to constrain the contribution from $\bar{K}^*\pi e\nu_e$, and find $B(D^+ \rightarrow \text{all } \bar{K}^*\pi e^+\nu_e) < 1.2\%$.

CONCLUSION

Combining the two results for $B(D^+ \rightarrow \text{all } \bar{K}^*\pi e^+\nu_e)$, we find a limit of 1.2% at 90% confidence level, which is

restricted by the $\bar{K}^0\pi^+\pi^-e^+\nu_e$ result. For nonresonant decays, or other resonances such as $K\rho e\nu_e$, $B(D^+ \rightarrow K^-\pi^+\pi^0e^+\nu_e) < 0.6\%$ and $B(D^+ \rightarrow \bar{K}^0\pi^+\pi^-e^+\nu_e) < 0.5\%$ are found. These two limits constrain the branching ratio for all $\bar{K}\pi\pi$ decays to be $B(D^+ \rightarrow \text{all } \bar{K}\pi\pi e^+\nu_e) < 0.9\%$. Earlier results on these decays come from the Lexan Bubble Chamber-European Hybrid Spectrometer (LEBC-EHS) experiment NA27 [8]: $B(D^+ \rightarrow \bar{K}^0\pi^+\pi^-e^+\nu_e) = (2.2^{+4.7}_{-0.6})\%$ and $B(D^+ \rightarrow K^-\pi^+\pi^0e^+\nu_e) = (4.4^{+7.3}_{-1.3})\%$. In Table II we give a summary of $D^+ \rightarrow \bar{K}\pi\pi e^+\nu_e$ and $D^+ \rightarrow \bar{K}^*\pi e^+\nu_e$ branching-ratio limits at the 90% confidence level. Using the E691 value for the D^+ lifetime, we find $\Gamma(D^+ \rightarrow \text{all } \bar{K}^*\pi e^+\nu_e) < 1.1 \times 10^{10} \text{ s}^{-1}$ and $\Gamma(D^+ \rightarrow \bar{K}\pi\pi e^+\nu_e) < 0.8 \times 10^{10} \text{ s}^{-1}$. Our results confirm the theoretical picture that the higher K^* resonances can contribute only a small fraction of the total semileptonic rate.

ACKNOWLEDGMENTS

We thank the staffs of all the participating institutions. This research was supported by the U.S. Department of Energy, by the National Science Foundation, by the Natural Sciences and Engineering Research Council of Canada through the Institute of Particle Physics, by the National Research Council of Canada, and by the Brazilian Conselho Nacional de Desenvolvimento Científico e Tecnológico.

- [1] Z. Bai *et al.*, Phys. Rev. Lett. **66**, 1011 (1991).
- [2] J. C. Anjos *et al.*, Phys. Rev. Lett. **62**, 1587 (1989).
- [3] J. C. Anjos *et al.*, Phys. Rev. Lett. **67**, 1507 (1991).
- [4] J. C. Anjos *et al.*, Phys. Rev. Lett. **62**, 722 (1989).

- [5] J. C. Anjos *et al.*, Phys. Rev. Lett. **65**, 2630 (1990).
- [6] J. R. Raab *et al.*, Phys. Rev. D **37**, 2391 (1988).
- [7] J. Adler *et al.*, Phys. Rev. Lett. **60**, 89 (1988).
- [8] M. Aguilar-Benitez *et al.*, Z. Phys. C **36**, 559 (1987).